Protonation Effects on the Structure and Homogeneous Charge Transport Dynamics of Solid State Osmium Bis(bipyridyl)tetrazine Chloride Films

Robert J. Forster*

National Center for Sensor Research, School of Chemical Sciences, Dublin City University, Dublin 9, Ireland

Tia E. Keyes*

School of Chemistry, Dublin Institute of Technology, Kevin St., Dublin 8, Ireland

Alan M. Bond

Department of Chemistry, Monash University, Clayton, Victoria 3168, Australia

Received: December 6, 1999; In Final Form: March 12, 2000

Mechanically attached solid state films of $[Os(bpy)_2\text{-}4\text{-}tet\text{-}Cl](ClO_4)$ have been formed on platinum microelectrodes (where bpy is 2,2′-bipyridyl and 4-tet is 3,6-bis(4-pyridyl)-1,2,4,5-tetrazine). Scanning electron microscopy reveals that films exist as an amorphous array of microscopically small particles. At relatively high scan rates, the voltammetric response of these films is reminiscent of that observed for an ideal reversible, solution phase redox couple. The film structure is not affected by voltammetric cycling in perchloric acid which protonates the unbound pyridine moiety of the tetrazine ligand. In contrast, the films become significantly more homogeneous when cycled in sodium perchlorate electrolyte and appear to become microcrystalline. Slow and fast scan linear sweep voltammograms have been used to provide an absolute determination of the fixed site concentration as 1.8 ± 0.05 and 1.6 ± 0.06 M and apparent diffusion coefficients of $(6.4 \pm 0.3) \times 10^{-11}$ and $(5.0 \pm 0.4) \times 10^{-11}$ $cm^2\ s^{-1}$ in 1.0 M $NaClO_4$ and $HClO_4$ electrolytes, respectively. Under semiinfinite linear diffusion conditions, the voltammetric peak current varies in a sigmoidal manner with the electrolyte pH *increasing* with *decreasing* solution pH. This response provides an estimate of 3.5 ± 0.1 for the pK_a of the pyridine moiety of the tetrazine ligand within the solid which is approximately 0.8 pH units higher than that found in aqueous acetonitrile solution.

Introduction

Protonation is a fundamental reaction in materials chemistry, biochemistry, and related fields. In particular, it plays an important role in the kinetics of chemical reaction, e.g., by contributing to the catalytic power of enzymes.[1] Beyond the issue of reaction dynamics and energetics, protonation can markedly affect the crystal structure of complexes,[2] macromolecules,[3,4] and supramolecular materials. This sensitivity of the crystal structure is especially pronounced in biological systems such as antibodies where differences in pH as small as 1.5 units can cause significant changes in the conformation of the residues. Furthermore, in crystal engineering, proton bridges are frequently used to form ordered supramolecular arrays in solid state materials, which have potential application in novel electrochemical or electrooptic devices.[2] However, despite this widespread importance, relatively few model systems exist that allow the effect of protonation on both the physical structure and reaction dynamics to be conveniently probed. Solid materials are typically characterized in their native or solid states using diffraction or spectrophotometric techniques. However, these approaches typically provide only indirect information about the impact of structural changes on the redox conductivity of a material. Therefore, approaches that allow the electrochemical properties of solids to be interrogated are becoming increasingly important.

Solution phase electrochemical studies have been common for many years. However, in recent times, studies in the solid state have grown in importance as a result of their relevance to photovoltaic cells, batteries, and other electrochemically based technologies.

Recently, a very versatile method of studying the voltammetry of solids has been developed in which microcrystals of solid are immobilized on an electrode surface, which is then placed in a solvent (electrolyte) medium.

Investigations into the voltammetry of water insoluble particles that are mechanically attached to electrode surface have demonstrated that nucleation and crystal growth phenomena can accompany redox switching.[5] Systems of this kind have been used to probe the dynamics of crystal growth, the effect of the charge, and structure of the complex on crystallization[6] as well as the dynamics of charge transport through the films.[7] In principle, when microcrystals are adhered to an electrode it becomes possible to have a model of charge transport that resembles behavior found in conducting polymers containing redox active centers.[8]

In this contribution, we present the voltammetry of microcrystals of $[Os(bpy)_2\text{-}4\text{-}tet\text{-}Cl](ClO_4)$ (Chart 1) (where bpy is 2,2'-bipyridyl and 4-tet is 3,6-bis(4-pyridyl)-1,2,4,5-tetrazine) that are mechanically attached to macro- and microdisk electrodes. The complex is insoluble in water, allowing the solid state redox properties to be probed by placing the modified electrode in an aqueous electrolyte media. From the perspective of investigating the effect of protonation, the tetrazine ligand of the complex contains an unbound pyridine moiety that is

10.1021/jp994275g CCC: $19.00
Published on Web 06/17/2000

CHART 1

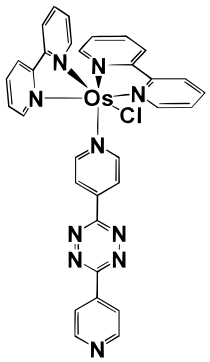

capable of undergoing protonation/deprotonation depending on the pH of the contacting electrolyte. Thus, it is possible to probe the effect of protonation on both the film structure and the charge transport mechanism through the microcrystals.

In contrast to other solid state films, this material exhibits exceedingly well-defined metal-based oxidation processes across a wide range of electrolyte pHs, making them attractive model systems for investigating the dynamics of charge transport through films. It is well-known that osmium polypyridyl complexes undergo fast electron self-exchange reactions. However, the situation in solid films can be complicated by the ion movement necessary to maintain electroneutrality. In this study, we have used microelectrodes[9−12] at long (tens of seconds) and short (tens of milliseconds) time scales to determine both the concentration of redox active sites within the film and the rate of homogeneous charge transport. Although these solids transport anions to some extent, it appears that diffusion of perchlorate anions through the films in order to maintain electroneutrality dictates the overall rate of homogeneous charge transport. The diffusion-controlled current observed in cyclic voltammetry as a function of the electrolyte pH has been modeled using the Henderson−Haselbalch equation to obtain an effective pK_a for the pyridine moiety of the tetrazine ligand in the solid state.

These detailed investigations into the processes that dictate the crystallinity of solid state coatings, as well as, their electronic and ionic conductivity will underpin developments in crystal engineering, and in the development of materials for solid state applications such as light-emitting electrochemical cells and diodes,[13,14] chemical sensors,[15] charge storage and molecular electronics devices.[16,17]

Experimental Section

3,6-Bis(4-pyridyl)-1,2,4,5-tetrazine, (4-tet). 4-Cyanopyridine (52 g, 0.5 mol) and hydrazine monohydrate (25 g, 0.5 mol) were combined and heated to 100 °C for 5 h. The resulting yellow solid was collected after cooling and recrystallized from in hot ethanol/water, 2:1, v/v. This was then stirred for 2 h in ethanol with a slight excess of 2,3-dichloro-5,6-dicyano-1,4-benzoquinone at room temperature. The resulting bright pink solid was then collected and recrystallized as described. Yield, 10 g, (8%). Mp 244−246 °C, CHN, (Calcd. For $C_{12}H_8N_6$; C: 61.02%; H: 3.39%; N: 35.59%. Found C: 60.69%; H: 3.28%, N: 35.01%, (200 MHz) ^{1}H NMR data [CD_3CN]: H^2, H,[6] $H^{2'}$, $H^{6'}$, 8.92 ppm (m) (4H), H^3, H^5, $H^{3'}$, $H^{5'}$, 8.48 ppm (m).

[Os(bpy)$_2$-4-tet-Cl]ClO$_4$. 4-tet (0.12 g, 0.51 mM) was dissolved in 20 cm^3 of ethylene glycol and heated to reflux. *cis*-Os(bpy)$_2$Cl$_2$ (0.257 g, 0.45 mM) was dissolved in ethylene glycol and added to the refluxing solution over 20 min. The reaction mixture was allowed to reflux for a further 4 h. After cooling, a solution of concentrated aqueous $NaClO_4$ was added. The resulting solid (0.322 g, 82% yield) was collected by filtration and recrystallized from acetone/water (1/1 v/v). The purity of the complex was confirmed by CHN, (Calcd. For $OsC_{32}H_{24}N_{10}Cl_2O_4$; C: 43.98%; H: 2.74%; N: 16.03%. Found C: 43.21%; H: 2.84%, N: 16.31%) and HPLC. (200 MHz) ^{1}H NMR data [CD_3CN]: bipyridyl, H_3, 8.47−8.52 (d); H^4 (t), 7.84−7.86; H^6 (d), 7.62−7.64; H^5 (t), 7.28−7.32; 4-tet, H^2, 7.70 (d); H^3, 7.60 (dd); H^5 7.60 (dd); H^6, 7.70; $H^{2''}$,7.98 (dd); $H^{3''}$ 8.75 (d); $H^{5''}$, 8.75 (d); $H^{6''}$, 7.98.

Instrumentation. Microelectrodes were prepared using platinum microwires of radii between 1 and 12.5 μm sealed in glass shrouds that were mechanically polished and electrochemically cleaned as described previously.[18] All potentials are quoted with respect to a BAS Ag/AgCl gel-filled (saturated KCl) reference electrode. The potential of the ferrocene/ferricenium couple dissolved in acetonitrile containing 0.1 M TEAP as supporting electrolyte was +0.322 V. Cyclic voltammetry was performed using a CH Instruments model 660 Electrochemical Workstation. All electrolytes were thoroughly degassed using nitrogen, and a blanket of nitrogen was maintained over the cell during all experiments.

All electrochemical measurements were carried out at room temperature, 293 °C, for solid state voltammetric measurements[19] two methods were used to transfer the solid onto the surface of the working electrode. In the first approach, the solid was transferred from a filter paper onto the surface of the working electrode by mechanical abrasion. This process caused some of the complex to adhere to the electrode surface as a random array of particles. In the second approach that was used to achieve surface coverages greater than approximately 10^{-7} mol cm^{-2}, a drop of Milli-Q water was first added to the complex before transferring the material onto the electrode surface as a paste. Prior to electrochemical measurements, the coating was allowed to dry. Beyond minor differences in the initial scans, films prepared by both methods give indistinguishable voltammetric responses. The stability of the films prepared by the two methods toward dissolution is comparable. After use, the electrode surface was renewed by polishing using an aqueous slurry of 0.3 μm alumina.

Scanning electron microscopy (SEM) was performed using a Hitachi S-3000N system. For SEM investigations, films were formed on 3 mm radius graphite disks that were mounted directly in the microscope. In electrochemical investigations, the modified disks were electrochemically cycled and then the layers were allowed to soak in electrolyte free Milli-Q water for at least 20 min before being washed copiously and then dried in a vacuum desiccator for several hours.

Raman spectroscopy was conducted on a Dilor.Jobiny-von.Spex Labram. The exciting 20 mW helium−neon laser (632.8 nm) was focused through a purpose made electrochemical cell onto the mechanically attached sample on a gold electrode surface using a 10× objective lens. The beam diameter when focused is approximately 1 μm producing approximately 106 W cm^{-2} at the sample. Focusing was confirmed by using a CCD camera in imaging mode. A spectral resolution of 1.5 cm^{-1} per pixel was achieved using a grating of 1800 lines/mm. The applied potential was controlled with respect to an SCE reference electrode using a CH instruments model 600A potentiostat.

The pK_a of [Os(bpy)$_2$(4-tet)Cl]$^+$ was determined from UV−visible spectra recorded on a Shimadzu UV-2101PC spectrophotometer. Titrations in the pH range 1−8 were conducted in a Britton Robinson buffer, 0.04 M H_3BO_3, 0.04 M H_3PO_4, and 0.04 M CH_3COOH. The pH was controlled by addition of

aliquots of concentrated HCl and NaOH. Spectroscopic changes were confirmed to be reversible by first decreasing and then increasing the solution pH between 1 and 7.5. Irreversible spectroscopic changes were observed at pHs greater than approximately 10. The pK_as were determined by fitting the spectroscopic changes occurring at 510 nm to the Henderson−Hasselbalch equation using nonlinear optimization procedures. The error on the pK_a values is approximately ±0.2.

Results and Discussion

General Electrochemical Properties. When the redox composition of an immobilized layer is switched, charge-compensating counterions must move into or out of the layer in order to maintain electroneutrality. Moreover, in the case of solid films that are mechanically attached onto an electrode surface, it is possible that the physical state of the layer, e.g., crystallinity, may change in response to changes in the oxidation state of the material. Therefore, an important objective is to probe whether "break-in" phenomena, such as changes in peak shape and position or the appearance of "inert zones",[20] are observed when a freshly deposited layer is subjected to voltammetric cycling. To address this issue, we have used scanning electron microscopy to examine changes in the physical structure of the layers before and after voltammetric cycling on glassy carbon disks. Comparison of the voltammetric behavior of $[Os(bpy)_2\text{-4-tet-Cl}]ClO_4$ on platinum and glassy carbon revealed that the general features of the electrochemistry are the same on each electrode type. Figure 1A shows that a mechanically attached film of $[Os(bpy)_2\text{-4-tet-Cl}]ClO_4$ on glassy carbon exists as a powder of micron or submicron dimensions before electrochemical cycling. Figure 2 shows the voltammetric response obtained when a similar layer formed on a 5 μm radius platinum microdisk is repeatedly cycled between −0.2 and +0.9 V in 1.0 M $NaClO_4$ so as to trigger the metal based $Os^{2+} \rightleftharpoons O^{3+}$ redox reaction. This figure shows that the anodic peak current decreases by approximately 30% over the initial 20 scans before reaching an equilibrium value that remains constant to within experimental error for several thousand scans. This initial decrease in the peak current is observed for $50 < \nu \leq 2000$ mV s^{-1}, suggesting that a following chemical reaction is not responsible for the observed behavior. That the most significant changes occur in the anodic branch suggest that the decrease in current observed may be linked to transport of charge compensating perchlorate into the film. However, it is possible that the oxidized from of the complex is more soluble and that some of the weakly attached material is lost from the electrode surface when it is first exposed to the electrolyte solution.

The voltammetric response observed after 50 repetitive scans is similar to that expected for an ideal reversible redox reaction that is controlled by a semiinfinite linear diffusion process; i.e., the ratio of the anodic to cathodic peak currents is unity and the peak currents increase linearly with the square root of the scan rate, ν. This behavior is unusually ideal for layers of this type and suggests that the film exists as a rather porous solid through which charge compensating counterions are relatively mobile. However, the peak-to-peak separation, ΔE_P (120 mV) is larger than the 56 mV expected for a reaction involving the transfer of a single electron. The behavior is somewhat less ideal than the associated solution phase electrochemistry where the metal oxidation for the deprotonated complex is observed at 0.166 V vs SCE in acetonitrile containing 0.1 M TBAF as supporting electrolyte where ΔE_p is 66 mV.

We have recorded SEM images after the solid state films have been repeatedly cycled on glassy carbon for up to 2000 scans at 50 mV/s. Under these conditions, the peak current, shape, and position remain unchanged between successive scans. The SEM images reveal that while repetitive cycling reduces both the absolute size of the individual particles within the film and range of particle sizes, the majority (≈80%) of the film remains in a noncrystalline state even after 2000 voltammetric

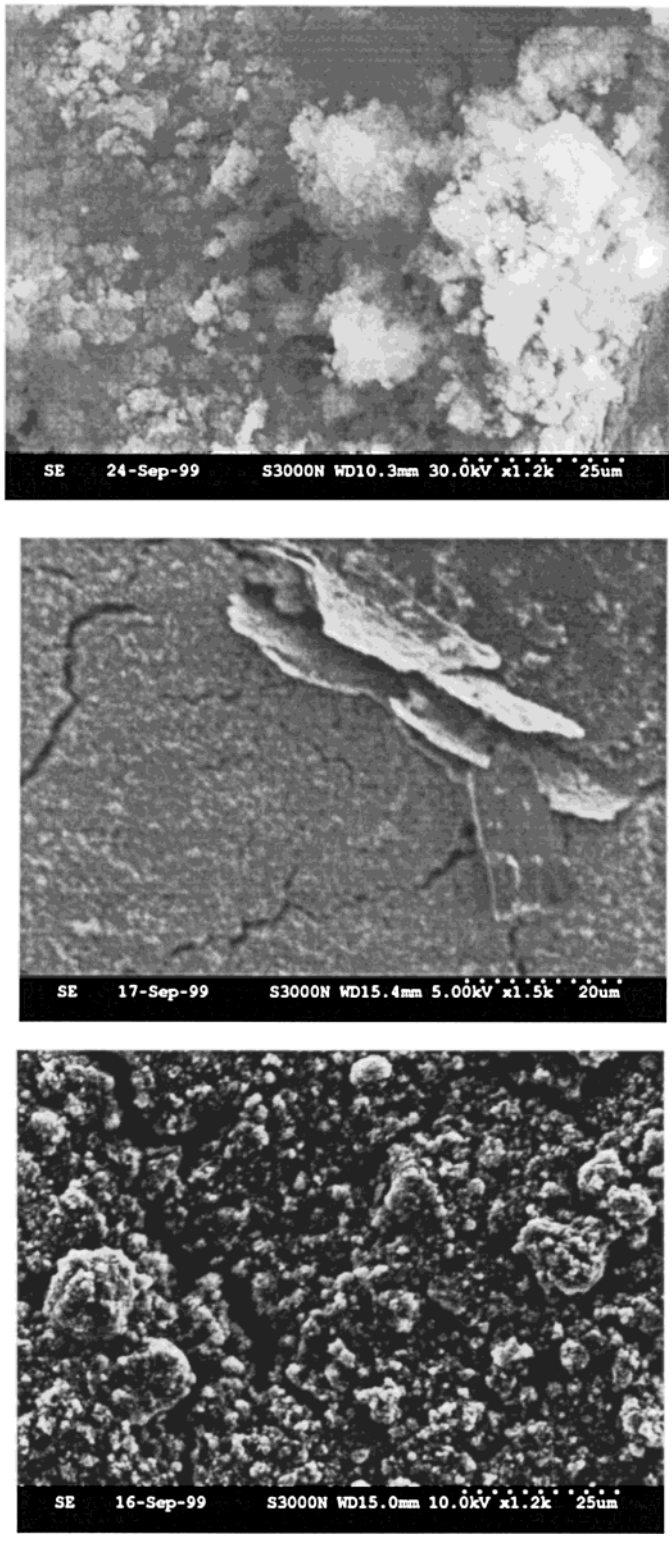

Figure 1. Scanning electron microscopy images of 3 mm radius graphite disks modified with a mechanically attached $[Os(bpy)_2\text{-4-tet-Cl}]ClO_4$ film powder as synthesized (A, top). (B, middle) and (C, bottom) are images after 1000 voltammetric cycles between −0.200 and +0.800 V at a scan rate of 50 mV s^{-1} in (B) 1.0 M $NaClO_4$ and (C) 1.0 M $HClO_4$.

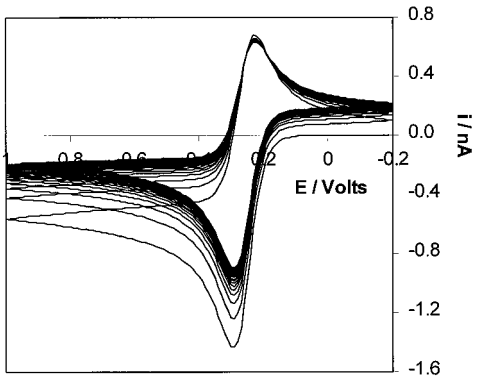

Figure 2. Effect of repeated scanning on the voltammetric response of an $[Os(bpy)_2\text{-4-tet-Cl}]ClO_4$ film that is mechanically attached to a 5 μm radius platinum microelectrode. The supporting electrolyte is 1.0 M $NaClO_4$ and the scan rate is 50 mV s^{-1}. On the basis of the initial scan the surface coverage is approximately 5.5×10^{-8} mol cm^{-2}. The arrows indicate the change in peak current and potential during repetitive scanning. Anodic currents are down and cathodic currents are up.

scans. However, as shown in Figure 1B, there are small regions of the film in which microcrystalline plates of the osmium complex protrude from the electrode surface.

Given that these films exist as discrete particles, at least prior to voltammetric cycling, it is important to determine what percentage of the film is electrochemically active in order to determine the extent to which individual particles are interconnected. Given that the voltammetric response illustrated in Figure 2 corresponds to approximately 40 pg of material, it is not possible to use microelectrodes for measurements of this nature. However, we have transferred known quantities of the complex in the form of an aqueous suspension onto the surface of a 2.25 cm^2 gold electrode and allowed them to dry. Indistinguishable voltammetric responses were observed if the complex was transferred by mechanical abrasion of the electrode over a dry sample of the powder or the aqueous suspension approach were employed. The data obtained suggest that close to 100% of the immobilized layer is electrochemically active. For example, several layers have been formed by transferring 0.100 ± 0.01 mg of the material onto the 2.25 cm^2 electrode which is then voltammetrically cycled until a steady state response is obtained. The charge recorded using bulk electrolysis at +0.700 V is $(1.01 \pm 0.07) \times 10^{-3}$ C; i.e., 80−90% of the redox centers are electrochemically active under equilibrium conditions. Spectroscopic data (vide infra) supports this conclusion.

The charge, Q, recorded in bulk electrolysis experiments, or the areas under slow scan rate cyclic voltammograms, can be used in conjunction with eq 1 to determine the surface coverage, Γ, of electroactive redox centers:

$$\Gamma = Q/nFA \qquad (1)$$

where F is Faraday's constant and A is the area of the electrode. The surface coverage at a platinum microdisk electrode for the data presented in Figure 2 is 5.5×10^{-8} mol cm^{-2}. The saturation coverage for monolayers in a closely related system[21] is 1×10^{-10} mol cm^{-2}; in the films considered here, the surface coverage of 5.5×10^{-8} mol cm^{-2} is estimated to be equivalent to approximately 500 monolayers.

In conclusion, that nearly ideal reversible responses are observed in close to neutral pH electrolyte and that close to 100% of the redox centers are electrochemically active suggests that there is a high degree of interconnectivity between the individual particles.

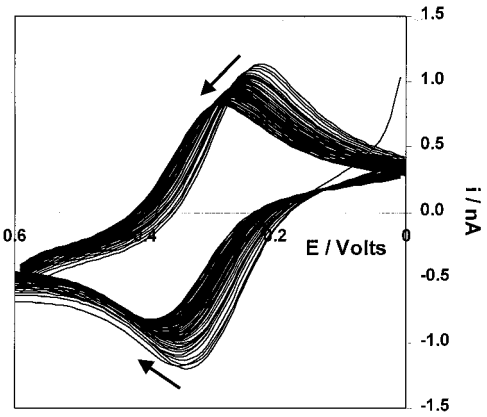

Figure 3. Effect of repeated scanning on the voltammetric response of an $[Os(bpy)_2\text{-4-tet-Cl}]ClO_4$ film that is mechanically attached to a 5 μm radius platinum microelectrode. The supporting electrolyte is 1.0 M $HClO_4$ and the scan rate is 50 mV s^{-1}. On the basis of the initial scan the surface coverage is approximately 5.5×10^{-8} mol cm^{-2}. The arrows indicate the change in peak current and potential during repetitive scanning.

Since the 4-tet ligand of the $[Os(bpy)_2\text{-4-tet-Cl}]ClO_4$ complex contains an unbound pyridine moiety capable of undergoing protonation/deprotonation reactions, solid state films of this material are attractive for probing how protonation affects the structure of the material and hence the voltammetric response. Figure 3 illustrates the voltammetric response observed in acidic electrolyte where the surface coverage is indistinguishable from Figure 2. In contrast to the unchanging peak potential found in near neutral pH electrolyte, the formal potential, $E^{\circ\prime}$, of the $Os^{2+/3+}$ couple shifts in a positive potential direction upon repeated cycling. This positive shift in $E^{\circ\prime}$ indicates that it becomes progressively more difficult to oxidize the film presumably as a result of the reduced electron-donating ability of protonated ligand or because of the higher overall positive charge on the protonated complex. This behavior is mirrored in the solution phase electrochemistry of these complexes where the metal oxidation potentials shift anodically by approximately 150 mV on protonation of the free pyridine. Protonation also influences the formal potentials observed for films that have been repeatedly cycled until the voltammetric response is unchanging, with values of 0.260 ± 0.020 and 0.360 ± 0.015 V being observed in 1.0 M $NaClO_4$ and 1.0 M $HClO_4$ electrolytes, respectively. Notwithstanding the shift in $E^{\circ\prime}$, the voltammetric response is close to ideal with $i_{p,a}/i_{p,c}$ equaling unity to within experimental error and ΔE_p being approximately 100 mV; this corresponds well with the solution phase ΔE_p which is also 100 mV. Figure 1C illustrates the SEM image obtained for the layer on glassy carbon after it has been cycled in 1.0 M $HClO_4$. This image is qualitatively similar to that found prior to voltammetric cycling suggesting that the changes in $E^{\circ\prime}$ observed during repetitive cyclic voltammetry do not correspond to a change in film morphology but arise because of slow protonation of the layer. Thus, it appears that the deprotonated complex can be electrocrystallized on the electrode surface but that protonation impedes crystallization presumably because of electrostatic repulsion within the solid.

Bulk Concentration and Homogeneous Charge Transport Rate. An important parameter that characterizes the structure of these films, and is essential for the accurate determination of apparent diffusion coefficients describing homogeneous charge transport through the layer (vide infra), is the concentration of redox centers within the film. As demonstrated previously by other researchers,[22−24] the voltammetric response observed at a microelectrode under different time regimes can be used to

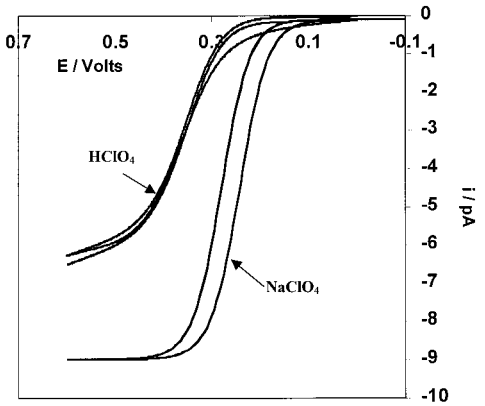

Figure 4. Steady state voltammograms recorded at 1 mV s^{-1} using a 2 μm radius microelectrode. The supporting electrolyte is 1.0 M $HClO_4$ and 1.0 M $NaHClO_4$ for the smaller and larger limiting currents, respectively.

determine the effective concentration of redox centers within solid state single crystals. Figure 4 shows the voltammetric responses of an $[Os(bpy)_2$-4-tet-Cl$]ClO_4$ film immobilized on a 2 μm radius platinum microelectrode ($\Gamma = (2.1 \pm 0.1) \times 10^{-7}$ mol cm^{-2}) recorded in 1.0 M $NaClO_4$ or 1.0 M $HClO_4$ at a scan rate of 1 mV s^{-1}. In this long time scale experiment, a steady state plateau current is observed, which is independent of the scan rate for $0.1 < \nu < 5$ mV s^{-1}. Moreover, Figure 4 shows that, although some hysteresis is observed in the case of 1.0 M $NaClO_4$, the currents observed in the forward and reverse scans are very similar. These results indicate that the response is predominantly controlled by a radial diffusion process. Under these slow scan rate conditions, the small size of the electrode becomes significant, the resulting spherical character of the diffusion field causes the mass transport process to be dominated by radial diffusion and the current attains a time independent steady state, i_{ss}, value which is provided by eq 2.

$$i_{SS} = 4nFD_{app}C_{eff}r \qquad (2)$$

where n is a number of electrons involved, D_{app} is the apparent diffusion coefficient describing homogeneous charge transport through the film, C_{eff} is the effective concentration of Os^{2+} centers within the film, and r is the radius of the microelectrode.

Our present data do not allow us elucidate the origin of the hysteresis observed in 1.0 M $NaClO_4$. However, given the relatively ideal voltammetric responses observed at high scan rate, it is unlikely to arise because of slow heterogeneous electron transfer across the electrode/film interface. That relatively little hysteresis is observed in 0.1 M $NaClO_4$, and that hysteresis is not observed in acidic electrolyte, suggests that in this long time scale experiment the film structure may change in response to changes in its oxidation state.

The inflection point of these sigmoidal shaped responses represents $E^{\circ\prime}$. In spite of the hysteresis observed at 1 M $NaClO_4$, Figure 4 confirms the previous observation that the formal potential of the $Os^{2+/3+}$ redox reaction depends on the nature of the supporting electrolyte. Moreover, that the limiting currents are larger for the $NaClO_4$ than for the $HClO_4$ electrolyte suggests that the diffusion coefficients and/or fixed site concentrations are not identical in the two circumstances.

The ability to establish a radial diffusion field in the slow scan rate experiments (Figure 4) impacts the accuracy of these fixed site concentrations and diffusion coefficients. In solution phase experiments, the experimental time scale is controlled through the scan rate so that thickness of the depletion zone is

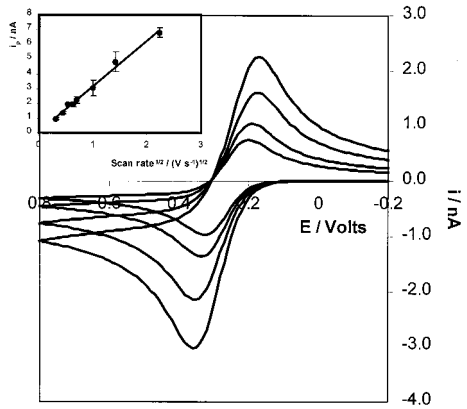

Figure 5. Scan rate dependence of the voltammetric response for a film of $[Os(bpy)_2$-4-tet-Cl$]ClO_4$ that is mechanically attached to a 5 μm radius platinum microelectrode. The supporting electrolyte is 1.0 M $NaClO_4$. From top to bottom, the scan rates are 1000, 500, 200, and 100 mV s^{-1}. Inset: i_p vs $\nu^{1/2}$ for films under these conditions.

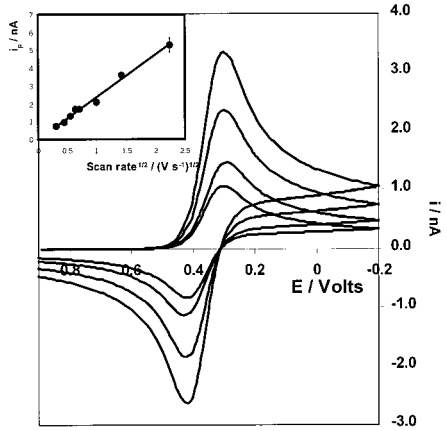

Figure 6. Scan rate dependence of the voltammetric response for a film of $[Os(bpy)_2$-4-tet-Cl$]ClO_4$ that is mechanically attached to a 5 μm radius platinum microelectrode. The supporting electrolyte is 1.0 M $HClO_4$. From top to bottom, the scan rates are 1000, 500, 200, and 100 mV s^{-1}. Inset: i_p vs $\nu^{1/2}$ for films under these conditions.

significantly larger than the electrode radius. This condition is difficult to meet for the solid state films investigated here because surface coverages larger than approximately 2×10^{-7} mol cm^{-2} adhere weakly to the electrode. For example, in the case of Figure 4, the layer thickness estimated using a fixed site concentration of 1.6 or 1.8 M is comparable to the radius of the microelectrode. However, that the limiting current observed is independent of scan rate between 0.1 and 5 mV s^{-1} suggests that the analysis is not significantly in error.

When the time scale of the voltammetric experiment is reduced such that the thickness of the depletion layer is significantly less than the film thickness, then the voltammetric response is controlled by a linear diffusion-like process and peak shaped voltammograms are observed. Figures 5 and 6 illustrate the voltammetric responses obtained in 1.0 M $NaClO_4$ and 1.0 M $HClO_4$ at scan rates between 100 and 1000 mV s^{-1} on a 5 μm microelectrode. Since peak-shaped responses are observed in which the peak current increases linearly as $\nu^{1/2}$, it appears that the diffusion field is small when compared to the radius of the ultramicroelectrode or to the thickness of the film.

While potential step methods are less sensitive to slow rates of heterogeneous electron transfer and ohmic loss,[25] cyclic voltammetry provides a convenient means of determining the reversibility of the system and can be used to easily measure apparent diffusion coefficients. For example, as illustrated in

TABLE 1: Effect of Sodium Perchlorate Concentration as Supporting Electrolyte on the Homogeneous Charge Transport Diffusion Coefficient through Solid State [Os(bpy)$_2$-4-tet-Cl]ClO$_4$ Films

[ClO_4^-]/M	$10^{11}D_{app}$/cm^2 s^{-1}	[ClO_4^-]/M	$10^{11}D_{app}$/cm^2 s^{-1}
0.1	2.7(0.1)	0.8	5.1(0.2)
0.2	3.2(0.1)	1.0	6.4(0.2)
0.6	4.4(0.3)		

the insets of Figures 5 and 6, for $100 \leq \nu \leq 1000$ mV s^{-1}, the voltammetric peak currents were directly proportional to the square root of scan rate. The cell resistance in these experiments is less than 200 Ω making the corresponding ohmic loss less than 1 mV. Under these circumstances, the peak currents can be described in terms of Randles−Sevçik equation:

$$i_p = 2.69 \times 10^5 n^{3/2} A D_{app}^{1/2} C_{eff} \upsilon^{1/2} \quad (3)$$

Therefore, the dependence of the voltammetric response on the apparent diffusion coefficient depends on the time scale of the experiment being directly proportional at long times, whereas a $D_{app}^{1/2}$ dependence is observed at short times. The absolute values of D_{app} and C_{eff} may be determined by using the experimental data in conjunction with eqs 2 and 3 and solving first for C_{eff} and then for D_{app}. This approach yields concentrations of 1.8 ± 0.05 and 1.6 ± 0.06 M and apparent diffusion coefficients of (6.4 ± 0.3) × 10^{-11} and (5.0 ± 0.4) × 10^{-11} cm^2 s^{-1} in $NaClO_4$ and $HClO_4$ electrolytes, respectively. These fixed site concentrations correspond to a radius of approximately 6.5 Å for the complex, which is in reasonable agreement with the crystallographic data of related polypyridyl complexes.[26] The decrease in concentration observed in $HClO_4$ is indistinguishable from that expected on the basis of the volume of perchloric acid that must be incorporated to fully protonate the film. This result suggests that electrostatic repulsion is not the major driving force for the increased inter-site separation found in the protonated solids.

Effect of Electrolyte Concentration on D_{app}. Table 1 contains the D_{app} values obtained as a function of the concentration of sodium perchlorate as supporting electrolyte. In the absence of an oxidation state dependent film structure, there are two dominant mechanisms that could limit the rate of homogeneous charge transport through these solid state films, namely electron hopping or counterion diffusion/migration. In the case of electron hopping, charge compensating counterions are freely available within the structure and D_{app} is expected to be at best weakly dependent on the electrolyte concentration. In contrast, Table 1 shows that D_{app} more than doubles on going from 0.1 to 1.0 M electrolyte suggesting that the rate of charge transport is limited by counterion movement. Moreover, even the maximum D_{app} value observed, 6.4 × 10^{-11} cm^2 s^{-1} would correspond to an electron self-exchange rate of 2.4 × 10^4 M^{-1} s^{-1} which is approximately 4 orders of magnitude smaller than the values typically reported for osmium polypyridyl complexes in solution[27] or within monolayers.[28−30] Therefore, we consider that the rate of charge transport through these films is limited by counterion motion.

Effect of Electrolyte pH on the Voltammetric Peak Currents. Because of its importance to a diverse range of areas including biological systems and chemical sensing, there is currently intense interest in the effect of protonation on electron transfer reactions in both the ground[31,32] and excited states.[33] By probing how the voltammetric peak current depends on the pH of the contacting electrolyte, these systems can provide an important insight into how the transition from solution to solid

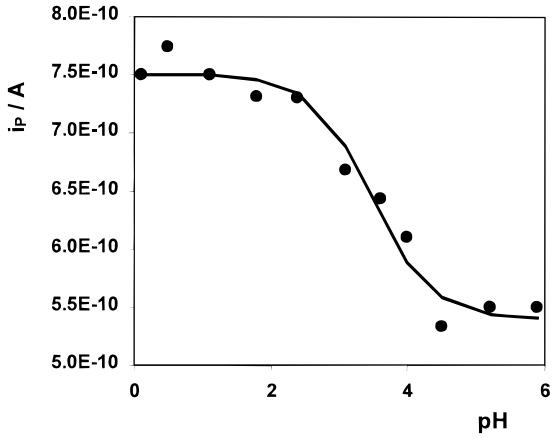

Figure 7. Dependence of the peak current observed for a film of [Os(bpy)$_2$-4-tet-Cl]ClO$_4$ that is mechanically attached to a 5 μm radius platinum microelectrode on the pH of the supporting electrolyte. The scan rate is 100 mV s^{-1}. The electrolyte solution contains 1.0 M $NaClO_4$ whose pH was adjusted by adding concentrated $HClO_4$.

states affects the pK_a. Figure 7 illustrates the dependence of the voltammetric peak current at 100 mV s^{-1} on the pH of the contacting electrolyte is systematically varied from approximately 0 to 6. Given that the voltammetric peak current is sensitive to the ionic strength, in these experiments the perchlorate concentration was kept constant at 0.1 M. The solution pH was adjusted by adding concentrated $HClO_4$ and the total perchlorate concentration was then adjusted to 0.1 M with $NaClO_4$. As the pH of the solution was adjusted, repetitive cyclic voltammograms were recorded until an unchanging peak current was obtained and all changes were confirmed to be reversible. The peak current increases in a sigmoidal manner from 0.55 to 0.75 nA as the pH is decreased from approximately 6 to 0. We have used nonlinear optimization in conjunction with the Henderson−Haselbalch equation to determine the apparent pK_a of the unbound pyridine moiety when it is immobilized within the solid film. The best fit line provided by this model is illustrated as a solid line in Figure 7, and the close correlation between theory and experiment suggests that the Henderson−Haselbalch equation provides an appropriate description of protonation in this system. The pK_a obtained is 3.5 ± 0.1 for the solid structure. Figure 8 shows the changes in the UV−visible spectrum that occur when the pH of the solution is systematically varied from approximately 6 to 1. These data indicate that the pK_a for the complex in aqueous buffer is 2.7 ± 0.2. The greater acidity of the pyridine nitrogen in aqueous solution is most likely due to the higher dielectric constant and greater solvating ability of the aqueous medium.[34]

Potential-Dependent Raman Spectroscopy. Potential-dependent Raman spectroscopy was carried out in order to identify the structural changes accompanying the redox chemistry of [Os(bpy)$_2$-4-tet-Cl]ClO$_4$. Raman has proven useful[35] as one of the few spectroscopic methodologies amenable to investigations of solid state electrochemistry. In the method described here, focusing of the laser on to the solid analyte was achieved using a microscope and imaging CCD camera, this approach eliminates any contribution to the Raman spectrum from background electrolyte or the electrode shroud.

Figure 9, a and b, shows the Raman spectra of solid [Os(bpy)$_2$-4-tet-Cl]ClO$_4$ immobilized on a gold electrode at −0.2 and 0.5 V vs SCE, respectively. From the spectroscopy of this complex, the exciting HeNe laser (632.8 nm) is expected to be preresonant with the MLCT (Os(II)-bpy π^*) transition and this is confirmed with the enhancement of features at 1604, 1550,

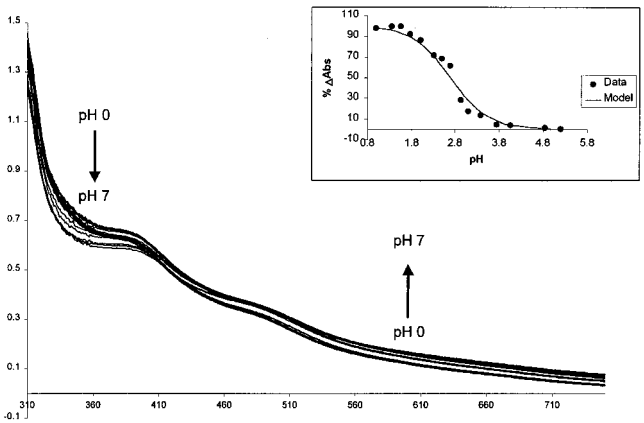

Figure 8. pH titration of $[Os(bpy)_2\text{-}4\text{-}tet\text{-}Cl]ClO_4$ in water:acetonitrile (90:10 v/v). pH is systematically varied from 1 to 7. The inset shows the change in absorbance observed at 500 nm and the best fit obtained to the Henderson−Haselbalch equation using a pK_a value of 2.69.

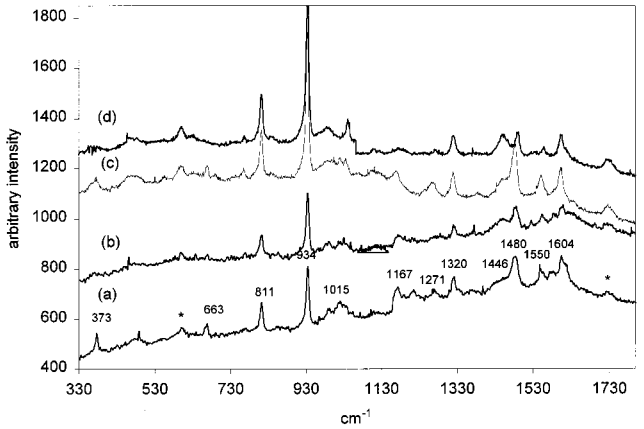

Figure 9. Potential controlled Raman spectra of $[Os(bpy)_2\text{-}4\text{-}tet\text{-}Cl]ClO_4$ mechanically attached to a gold disk electrode (a) −0.2V in 0.1 M $NaClO_4$, (b) 0.4 V in 0.1 M $NaClO_4$, (c) −0.2V in 0.1 M $HClO_4$, and (d) 0.4V in 0.1 M $NaClO_4$. All potentials are vs SCE, λ_{ex} 632.8 nm.

1480, 1320, 1268, 1167, and 1015 cm^{-1}, all associated with the bipyridyl moieties. A weaker feature at 373 cm^{-1} is associated with the Os−N stretch. Two very intense features at 811 and 934 cm^{-1} are attributed to surface enhanced transitions, possibly due to the tetrazine or its associated free pyridine. These bands are not observed when the bare solid is examined on glass or when the bare electrode is examined, but are observed when the material is observed on gold even at monolayer coverages. These bands appear to be largely unaffected by switching the oxidation state of the layer. Figure 9, a and b, illustrates the Raman spectra of the solid material at −0.2 and 0.5 V vs SCE in 0.1 M $NaClO_4$, respectively, while spectra c and d were recorded in 0.1 M $HClO_4$ electrolyte. In the latter solution, the pyridine group is expected to be fully protonated. From the pK_a titration shown in Figure 8, the exciting laser is no less preresonant with the MLCT band for the protonated compound and this is borne out in the similarity between the spectra a and c. The only significant difference between the acidic and neutral medium is the Os−N mode which has shifted to 383 cm^{-1} under acidic conditions. In each case, oxidation of the material results in loss of the low-frequency Os(II)−N vibration, consistent with metal oxidation. The significant loss of intensity observed in these bands suggests that the solid is completely oxidized, since Raman probes only the outermost layers of the solid material close to the layer/solution interface. Oxidation of the metal results in loss of MLCT and one might expect that the resonance condition would be lost. However, after oxidation the laser becomes preresonant with a bpy (π)−Os LMCT transition and the bpy-based bands continue to be observed even for the oxidized layers, albeit with different relative intensities. Therefore, the Os−N mode provides a suitable spectral marker for oxidation in these systems.

Conclusions

Mechanically attached solid state films of $[Os(bpy)_2\text{-}4\text{-}tet\text{-}Cl]ClO_4$, where bpy is 2,2′-bipyridyl and 4-tet is 3,6-bis(4-pyridyl)-1,2,4,5-tetrazine, have been formed on platinum microelectrodes. Scanning electron microscopy reveals that repeated voltammetric cycling in sodium perchlorate electrolyte can induce some crystallization of the material on the electrode surface. However, the voltammetric response does not indicate a nucleation and crystal growth process as reduced microcrystals are converted to oxidized microcrystals. In contrast, in perchloric acid the films remain amorphous even after several thousand voltammetric scans. In both electrolytes, the films can be reversibly switched between the Os^{2+} and Os^{3+} oxidation states with the electrochemical responses being close to ideal. At short experimental time scales, the cyclic voltammograms are similar to those observed for solution phase reactants and the current response is controlled by anion transport through the solid. In contrast, at long time scales, the current is controlled by a radial diffusion process. We have combined these two responses to determine the absolute concentrations of redox centers within the film (1.8 and 1.6 M for $NaClO_4$ and $HClO_4$ electrolytes, respectively) and the apparent diffusion coefficients for homogeneous charge transport (2.7×10^{-11} and 5.0×10^{-11} cm^2 s^{-1} for $NaClO_4$ and $HClO_4$ electrolytes, respectively). The dependence of the voltammetric peak current on the pH of the contacting electrolyte has been used to estimate the pK_a of the unbound pyridine moiety of the tetrazine ligand as 3.5 ± 0.1.

Acknowledgment. R.J.F. is pleased to acknowledge the continuing financial support of the Irish Science and Technology funding agency, Enterprise Ireland, under the Strategic Research Programme Grant ST/98/414. R.J.F. and T.E.K., gratefully acknowledge the generous loan of precious metals from Johnson Matthey. T.E.K. and A.M.B. acknowledge the financial support of Enterprise Ireland under the International Collaboration Programme (IC/1999/006).

References and Notes

(1) Warshel, A.; Papazyan, A. *Proc. Natl. Acad. Sci. U.S.A.* **1996**, *93*, 13665.
(2) Aakeroy C. B.; Seddon K. R. *Chem. Soc. Rev.* **1993**, *22*, 397.
(3) McPherson, A. *J. App. Cryst.* **1995**, *28*, 362.
(4) Cohen, Y.; Buchner, S.; Zachmann, H. G.; Davidov, D. *Polymer* **1992**, *33*, 3811.
(5) (a) Bond A. M.; Scholtz, F. *J. Phys. Chem.* **1991**, *95*, 7640. (b) Bond, A. M.; Scholtz, F. *Langmuir* **1991**, *95*, 7640.
(6) Fletcher, S.; Halliday, C. S.; Gates, D.; Westcott, M.; Nelson, G. *J. Electroanal. Chem.* **1983**, *159*, 267.
(7) Bruce, P. G., ed.; *Solid State Electrochemistry*; Cambridge University Press: Cambridge, UK, 1995.
(8) Lyons, M. E. G. *Electroactive Polymer Electrochemistry*; Plenum Press: New York, 1996.
(9) Forster, R. J. *Chem. Soc. Rev.* **1994**, 289.
(10) Forster, R. J. In *Encyclopedia of Analytical Chemistry*; Meyers, R., Ed.; Wiley: New York, 1999.
(11) Forster, R. J.; Keyes, T. E. *J. Phys. Chem. B* **1998**, *102*, 10004.
(12) Forster, R. J. *Phys. Chem. Chem. Phys.* **1999**, *1*, 1543.
(13) Yang, C.; He, G.; Wang, R.; Li, Y. *J. Electroanal. Chem.* **1999**, *471*, 32.
(14) Salaneck, W. R.; Stafstrom, S.; Bredas, J.-L. *Conjugated Polymer Surfaces and Interfaces*; Cambridge University Press: Cambridge, UK, 1996.
(15) Opekar, F.; Štulík, K. *Anal. Chim. Acta* **1999**, *385*, 151.
(16) Wrighton, M. S. *Science* **1986**, *231*, 32.

(17) Chidsey, C. E. D.; Murray, R. W. *Science* **1986**, *231*, 25.
(18) Forster, R. J.; Faulkner, L. R. *J. Am. Chem. Soc*. **1994**, *116*, 5444.
(19) Bond, A. M.; Marken, F. *J. Electroanal. Chem.* **1994**, *372*, 125.
(20) Bond, A. M.; Fletcher, S.; Symons, P. G. *Analyst* **1998**, *123*, 1891.
(21) Forster, R. J.; Keyes, T. E.; Vos, J. G. *Analyst* **1998**, *123*, 1987.
(22) Kulesza, P. J.; Faulkner, L. R. *J. Am. Chem. Soc*. **1994**, *115*, 5, 11878.
(23) Whiteley, L. D.; Martin, C. R. *J. Phys. Chem.* **1989**, *93*, 4650.
(24) Winlove, C. P.; Parker, K. H.; Oxenham, R. K. C. *J. Electroanal. Chem.* **1984**, *170*, 293.
(25) Bard, A. J.; Faulkner, L. R. *Electrochemical Methods, Fundamentals and Applications*; Wiley: New York, 1980.
(26) Juris, F.; Balzani, V.; Barigelletti, F.; Campagna, S.; Belser, P.; von Zelewsky, A. *Coord. Chem. Rev*. **1988**, *82*, 85.
(27) Chan, M. S.; Wahl, A. C. *J. Phys. Chem*. **1978**, *82*, 2542.
(28) Charych, D. H.; Majda, M. *Thin Solid Films* **1992**, *210*, 348.
(29) Charych, D. H.; Anvar, D. J.; Majda, M. *Thin Solid Films* **1994**, *242*, 1.
(30) Lee, W.-Y.; Majda, M.; Brezesinski, G.; Wittek, M.; Möbius, D. *J. Phys. Chem. B*, in press.
(31) Baitalik. S.; Florke, U.; Nag, K. *Inorg. Chem*. **1999**, *38*, 3296.
(32) O'Kelly, J. P.; Forster, R. J. *Analyst* **1998**, *123*, 1987.
(33) Geisser, B.; Ponce, A.; Alsfasser, R. *Inorg. Chem*. **1999**, *38*, 2030.
(34) Davilla, J.; Bignozzi, A.; Scandola, F. *J. Phys. Chem*. **1989**, *93*, 1737.
(35) Bond, A. M.; Marken, F.; Williams, C. T.; Beatty, D.; Keyes, T. E.; Forster, R. J.; Vos, J. G. *J. Phys. Chem*., in press.